photonics

MDPI

Communication

Effect of a Femtosecond-Scale Temporal Structure of a Laser Driver on Generation of Betatron Radiation by Wakefield Accelerated Electrons

Andrey D. Sladkov [1,2] and Artem V. Korzhimanov [1,2,*]

[1] Institute of Applied Physics of the Russian Academy of Sciences, 603950 Nizhny Novgorod, Russia
[2] Lobachevsky Faculty of Radiophysics, State University of Nizhny Novgorod, 603022 Nizhny Novgorod, Russia
* Correspondence: artem.korzhimanov@ipfran.ru

Abstract: The brightness of betatron radiation generated by laser wakefield accelerated electrons can be increased by utilizing the laser driver with shorter duration at the same energy. Such shortening is possible by pulse compression after its nonlinear self-phase modulation in a thin plate. However, this method can lead to a rather complex femtosecond-scale time structure of the pulse. In this work, the results of numerical simulations show that the presence of prepulses containing a few percent of the main pulse energy can significantly alter the acceleration process and lead to either lower or higher energies of accelerated electrons and generated photons, depending on the prepulse parameters. Simultaneously, the presence of a pedestal inhibits the acceleration process lowering the brightness of the betatron source. Furthermore, postpulses following the main pulse are not found to have a significant effect on betatron radiation.

Keywords: laser plasma interaction; wakefield electron acceleration; betatron radiation; X-ray source; femtosecond pulse; thin plate compression

Citation: Sladkov, A.D.; Korzhimanov, A.V. Effect of a Femtosecond-Scale Temporal Structure of a Laser Driver on Generation of Betatron Radiation by Wakefield Accelerated Electrons. *Photonics* **2023**, *10*, 108. https://doi.org/10.3390/photonics10020108

Received: 15 December 2022
Revised: 16 January 2023
Accepted: 17 January 2023
Published: 20 January 2023

1. Introduction

Soft X-ray sources are widely used in many applications [1,2]. One of the urgent modern problems is the creation of sufficiently bright sources of soft X-ray radiation for applications such as absorption X-ray radiography and phase-contrast X-ray imaging for biological and medical purposes [3–6]. As a rule, to generate bright radiation in this range, radiofrequency accelerators such as synchrotrons or linear accelerators, followed by an undulator, are used. However, to generate bright radiation in the range of 1–100 keV, electron beams with an energy of hundreds of MeV are required, which require the large size of conventional accelerators. Much more compact laser-plasma X-ray sources have been proposed as an alternative for those applications [7–9]. Among them, the most popular method of radiation generation in the required range is the so-called betatron source [10–12]. In this method, the X-rays are radiated by electrons simultaneously being accelerated and transversely oscillating in the plasma cavity behind an intense laser pulse propagating in underdense plasmas.

Despite the fact that the brightness of the betatron source was experimentally achieved at the level of 10^8–10^9 photons per shot, the problem of further increasing the brightness is still relevant [13]. One of the possible ways to increase the brightness for the same laser pulse energy can be to reduce the duration of the driving laser pulse.

Indeed, according to the widely accepted phenomenological model developed by Lu et al. [14], the width of the laser pulse w_0 should be consistent with its intensity, and a density of the plasma target due to a relation $(kw_0)^2 \approx 4a_0/n_0$, where k is a wavenumber of the laser pulse, $a_0 = eE_0/m\omega c$ is a relativistic amplitude (e—elementary charge, E_0—electric field amplitude of the laser pulse, m—electron mass, ω—laser frequency,

c—speed of light), $n_0 = e^2 N_e / \varepsilon_0 m\omega^2$ is a plasma overdense parameter (N_e—background electron concentration, ε_0—electrical constant). In this case, the energy gained by an electron in a plasma wake is scaled as $\gamma \approx 2a_0/3n_0$, where γ is the maximum achievable relativistic gamma factor of the accelerated electrons [14]. Let us fix the laser pulse energy: $W = W_{\text{rel}} a_0^2 (kw_0)^2 \omega\tau_0$, where $W_{\text{rel}} = \varepsilon_0 m^2 c^5 / 2e^2\omega$ ($W_{\text{rel}}[\text{J}] = 1.84 \times 10^{-7} \lambda[\mu\text{m}]$), τ_0 is the pulse duration, and find the dependence of the electron energy on the pulse duration and plasma density:

$$\gamma \approx \frac{1}{3}\left(\frac{2W}{W_{\text{rel}} n_0^2 \omega\tau_0}\right)^{1/3} \tag{1}$$

The power of the betatron radiation can be estimated from the following expression [11]:

$$P_b \approx \frac{e^2\omega^4}{12c^3}\gamma^2 n_0^2 r_b^2 \tag{2}$$

where r_b is the amplitude of betatron oscillations, which we will consider in accordance with the theory of ultrarelativistic similarity [15] as inversely proportional to the root of the plasma density: $r_b = n_0^{-1/2} r_{b0}$, where r_{b0} is a constant determined by the shape of the laser pulse. Then from (1) and (2) we obtain:

$$P_b \approx \frac{e^2\omega^4 r_{b0}^2}{108c^3}\left(\frac{2W}{W_{\text{rel}}}\right)^{2/3}\left(\frac{n_0}{(\omega\tau_0)^2}\right)^{1/3}. \tag{3}$$

From this it can be seen that, at the fixed energy and the duration of the laser pulse, the power of betatron radiation increases with increasing plasma density. However, as the plasma density increases, the plasma wavelength decreases, and when it becomes shorter than the pulse length, the acceleration efficiency drops sharply, so the most optimal is to use plasma with a density of $n_0 \approx 1/(\omega\tau_0)$ for which the pulse duration and the plasma wavelength are of the same order. In this case, we have the betatron radiation power equal to

$$P_b^{\text{opt}} \approx \frac{e^2\omega^3 r_{b0}^2}{108c^3\tau_0}\left(\frac{2W}{W_{\text{rel}}}\right)^{2/3} \tag{4}$$

Thus, at fixed pulse energy and an optimal choice of the plasma density and the laser pulse waist, the betatron radiation power increases with decreasing laser pulse duration.

Since it is possible to increase the brightness of betatron sources at the same energy of the laser pulse by shortening it, it seems promising to use the recently implemented scheme for compressing multiterawatt and petawatt laser pulses using nonlinear self-phase modulation in thin plates [16–22]. In this case, the pulse energy almost remains conserved, whilst its duration can be reduced several times. Under the best conditions, pulses with a duration of 11 fs at a power of 1.5 PW were achieved in this way [23]. The use of the pulses compressed by this method was also recently demonstrated experimentally to increase the brightness of betatron radiation [24]. However, as modeling shows, such pulses can have a rather complex temporal structure at femtosecond scales. In particular, a pulse can have a femtosecond pedestal and be accompanied by pre- and postpulses containing up to 20–30 % of the pulse energy. It was shown in [25] that the complex temporal structure of a pulse consisting of several pulses, i.e., the pulse with the precursor, can influence the size and form of the electron bunch formed and accelerated in the wakefield and therefore its betatron radiation. This work is devoted to the further analysis of this problem. We, however, restrict ourselves to the demonstrative analysis for a certain laser pulse parameters, leaving more general study for further works.

2. Methods

The analysis was carried out by numerical simulations by the fully electrodynamic Particle-In-Cell method using the PICADOR code [26]. The simulations were carried out in 2D geometry in a box 190×120 μm^2 in size. The size of the steps in the longitudinal

direction was $\Delta x = 0.05$ μm, and in the transverse direction it was $\Delta y = 1$ μm. The time step was $\Delta t = \Delta x/2c = 8.34 \times 10^{-2}$ fs.

A laser pulse with a wavelength of 900 nm and polarized in the out-of-plane z direction was generated at the left boundary. The pulse had a Gaussian transverse profile with a radius of 10 μm at the level $1/e$ of the amplitude, which corresponds to a focusing spot waist of 11.8 μm at FWHM (full width at half maximum) of the intensity. The longitudinal profile of the pulse varied; however, the total energy of the pulse was kept to be constant and equal to 1.73 J which gives the power equal to 1.15 TW, which roughly corresponds to the parameters obtained experimentally [24].

Plasma was assumed to be homogeneous with an electron concentration equal to 1.24×10^{19} cm^{-3}, which corresponds to the overdense parameter $n_0 = 0.009$. The plasma boundary was initially located at a distance of 10 μm from the left boundary of the box.

To reduce the calculation time, the moving window technique was used. Window movement began at the time instant $t = 570$ fs after the beginning of the calculation, which corresponded to the position of the laser pulse front at a distance of 150–170 μm from the left boundary. The speed of window movement was equal to the speed of light. The total calculation time was up to 8 ps.

Betatron radiation was calculated using the Monte Carlo method using the expressions for synchrotron radiation, as described in the paper [27].

3. Results

First, we carried out a simulation with a pure Gaussian 11-fs pulse. Here and below, the duration was determined at FWHM of the intensity. Thus, the dimensionless pulse amplitude was $a_0 = 7.5$ and its intensity was equal to 4.9×10^{19} W/cm^2.

The simulation results are shown in Figure 1. It can be seen that the laser pulse forms a plasma cavity behind it which capture a bunch of electrons and accelerate them to the energies of the order of 100 MeV. The cavity grows with time, capturing and accelerating more and more electrons. Overall structure of the cavity and the captured electron bunch becomes quite complex however the prominent generation of the photons in 10–100 keV range is seen. Those photons are emitted by high-energy electrons in the bunch which are transversely oscillating in plasma fields of the cavity. It also can be pointed out that at 5 ps the laser pulse almost extincts converting its energy in the energy of the plasma wake and accelerated electrons.

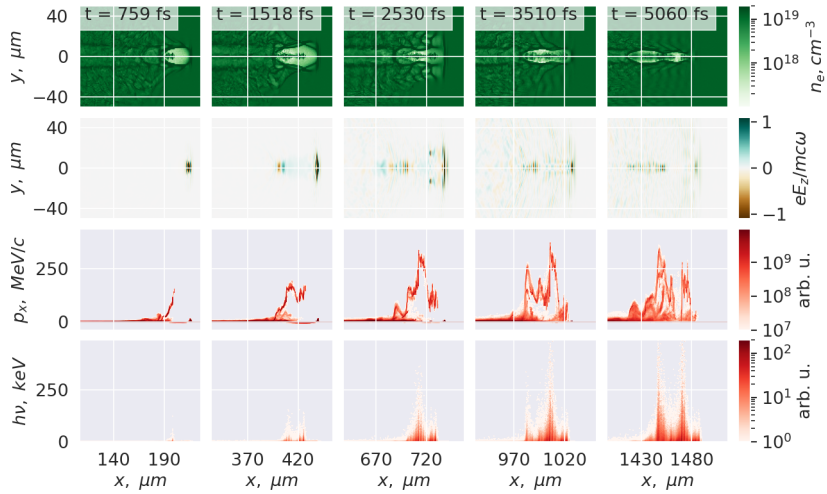

Figure 1. Simulation results for a Gaussian laser pulse with a duration of 11 fs. First row—electron density distribution, second row—out-of-plane electric field distribution (it corresponds to the laser pulse field), third row—electron phase space, fourth row—photon phase space. Columns refer to different instants of time shown at top left corners of the first row plots.

This can be better seen from the time dependence of the electron and photon spectra shown in Figure 2. The electron energies as well as photon energies significantly grow only until $t \approx 3$–4 ps after which the acceleration process effectively stops because of extinction of the laser pulse. It should be noted that this is also the moment of time when the front of the accelerated electron bunch reaches the front of the cavity as seen from the left panel of Figure 2. That is because the density of the plasma was chosen optimally such that the length of the pulse energy extinction and the length of the electrons overcoming the laser pulse were equal. Based on this the 4 ps simulation duration was chosen to be optimal and was used for spectra comparison in the following analysis.

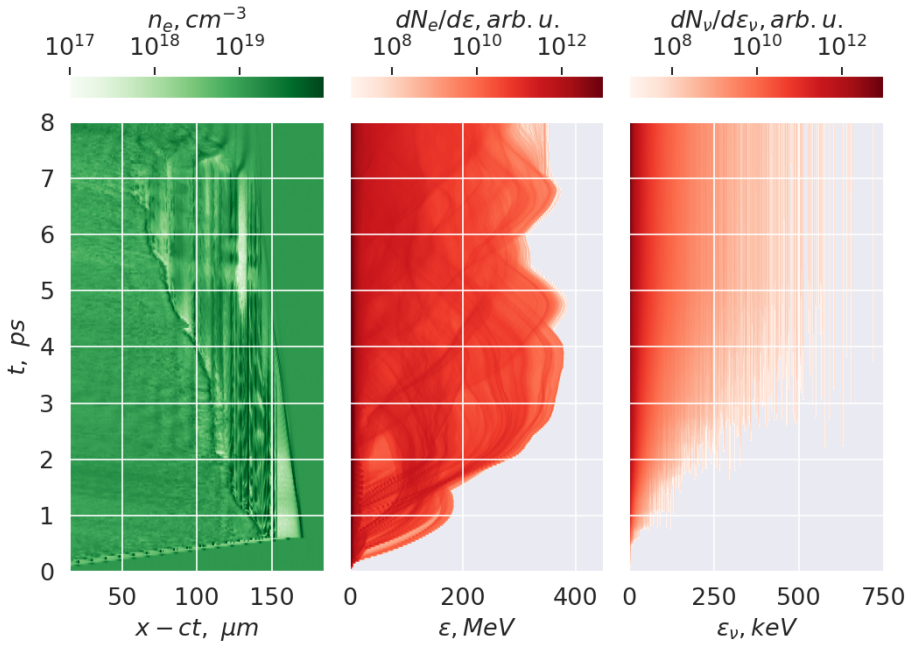

Figure 2. Simulation results for a Gaussian laser pulse with a duration of 11 fs. Spatiotemporal dynamics of electron density at $y = 0$ (**left**), time dependence of generated electron spectra (**center**), time dependence of generated photon spectra (**right**).

In order to confirm that the use of a shorter laser pulse increases the brightness of the betatron source, we compared the case of an 11-fs pulse with a case of a 50-fs pulse of the same energy. We adjusted plasma density in the latter case in order to satisfy optimal parameters according to the theory. So the electron concentration in this case was equal to 5.8×10^{18} cm^{-3}, which corresponds to the overdense parameter $n_0 = 0.0042$. The results of the simulations are shown in Figure 3. Comparing to the case of 11-fs pulse, the electrons are accelerated to roughly the same energies; however, their number is much lower due to lower density of the target. The energy of generated photons are also significantly lower due to weaker plasma fields in the wake. As a result, the generated radiation spectra is much narrower, which confirms the idea that the shortening of the laser pulse can enhance the betatron radiation.

Next, we studied the influence of a femtosecond scale prepulse on the acceleration process. Both the main pulse and the prepulse in these calculations had Gaussian shapes. The pulse duration was 11 fs and the prepulse duration was 5 fs. The prepulse preceded the pulse with a fixed delay equal to 27 fs. The amplitude of the prepulse varied in the range from $a_0 = 0.8$ to $a_0 = 3.6$ and the pulse amplitude varied accordingly so that the total energy of the laser radiation was constant and equal to 1.73 J.

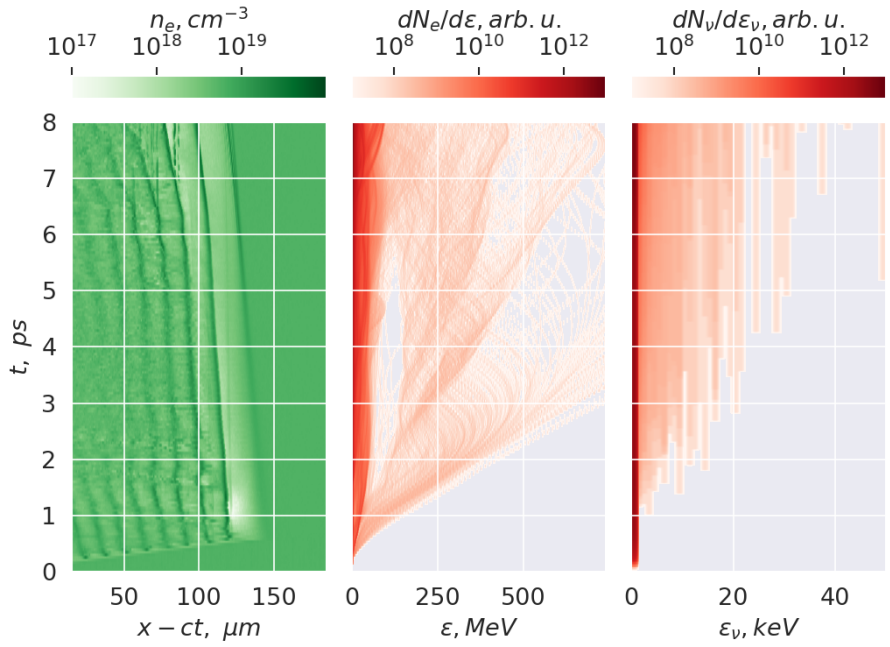

Figure 3. Simulation results for a Gaussian laser pulse with a duration of 50 fs. The data shown are similar to those in Figure 2. Note, however, that there are different scales for energies.

The final photon spectra obtained in these calculations are shown in Figure 4. It can be seen that a prepulse with a non-relativistic amplitude has little effect on the generated spectrum. The stronger prepulses, however, can alter the spectrum significantly either enhancing or inhibiting it. Say, the prepulse with the amplitude $a_0 = 1.6$ leads to increase in maximal photon energies from 400 to 500 keV to 600–700 keV and the prepulse with the amplitude $a_0 = 3.6$ leads to its decrease down to 150–200 keV. The brightness of the source is also influenced by the prepulses. For example, the number of 100 keV photons is several times higher in the case of the prepulse with the amplitude $a_0 = 1.6$ than in the case without prepulse and about 10 times lower in the case of the prepulse amplitude $a_0 = 3.6$.

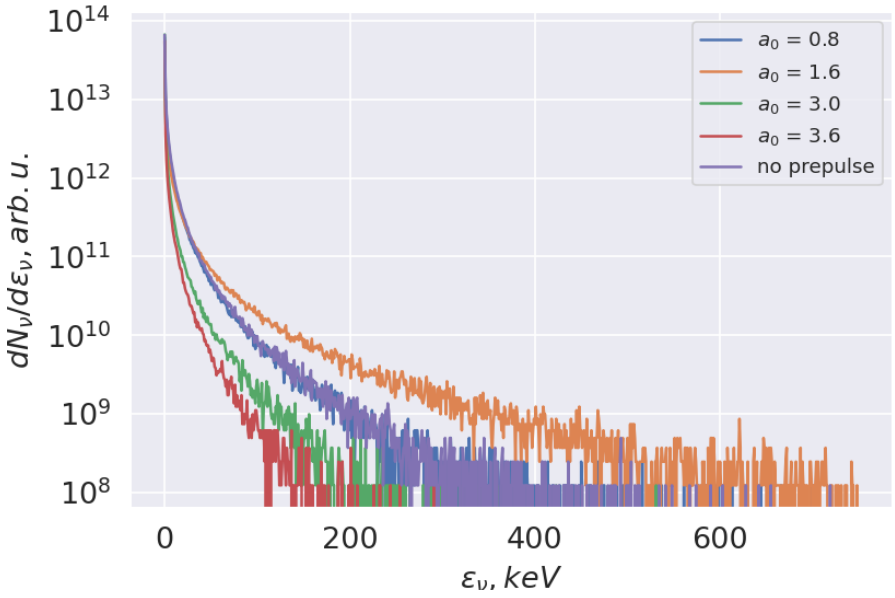

Figure 4. Comparison of photon spectra obtained from the simulations for 11 fs laser pulses with 5 fs prepulses with different amplitudes.

To understand the physical mechanisms behind observed spectra dependence on the prepulse amplitude, we analyzed dynamics of the interaction for different prepulses. Figure 5 shows the simulation results for the case where the radiation spectrum is wider and its intensity is higher (the prepulse amplitude $a_0 = 1.6$).

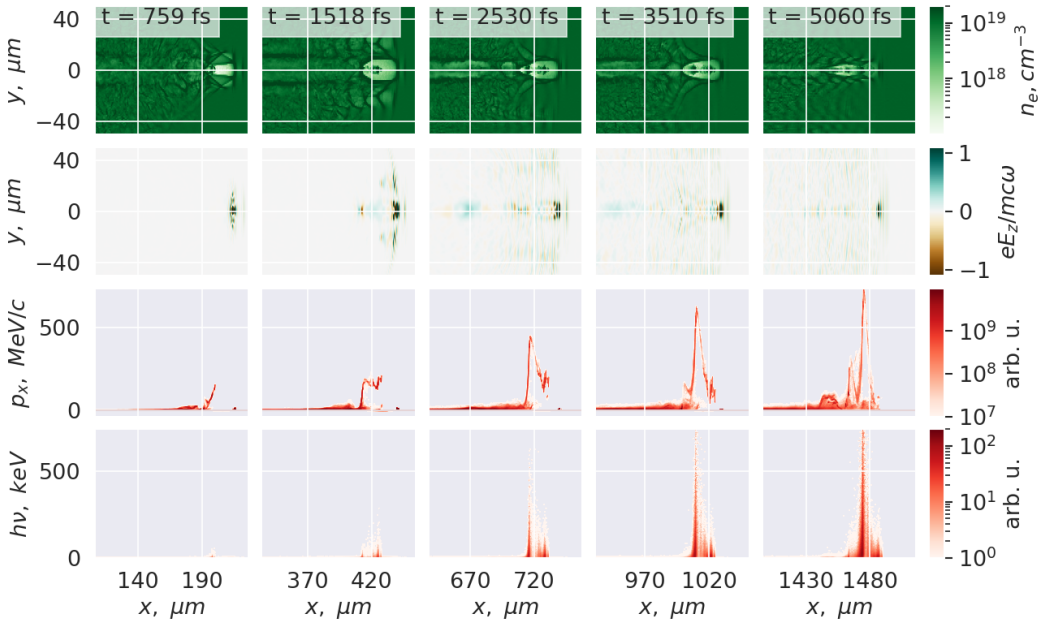

Figure 5. Simulation results for a Gaussian laser pulse with a duration of 11 fs with a 5-fs prepulse. The amplitude of the main pulse is $a_0 = 7.1$ and the amplitude of the prepulse is $a_0 = 1.6$. The data shown is similar to Figure 1. Note, however, the different scales of the electron momentum and photon energy.

The main difference with the case of pure pulse is that the prepulse forms a distinct electron channel in front of the main pulse, however, it does not deplete the electrons completely. This can be better seen from Figure 6 where lineouts in two perpendicular cross-sections are shown for different cases.

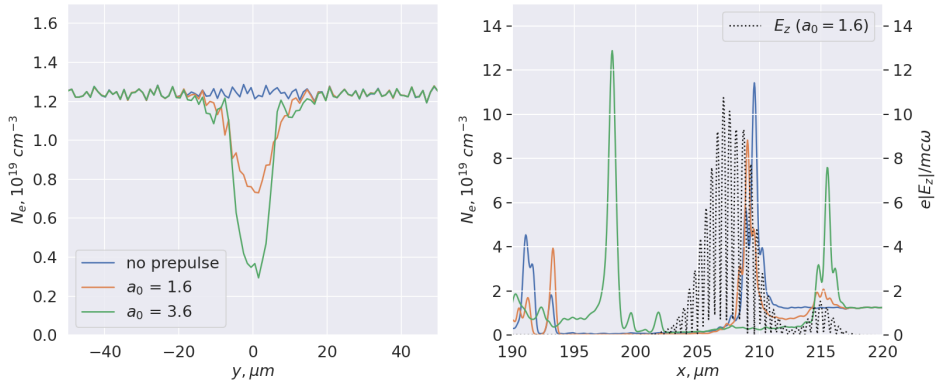

Figure 6. Lineouts of electron density in cross-sections $x = 212$ μm (**left**) and $y = 0$ (**right**) at time instants $t = 759$ fs in cases with different prepulse amplitudes a_0. On the right the shape of the laser pulse in the case of $a_0 = 1.6$ is shown for reference.

The main pulse effectively propagate in a preformed channel which leads to a more stable structure of the cavity. So the structure of the accelerated bunch is also more stable and there is only one distinct bunch accelerated to high energies. As a result, the attained energies of the electrons are higher and so they emit more photons with higher energies as well.

In contrast, Figures 6 and 7 show the simulation results for the case when the radiation spectra are narrower and its intensity is lower (the prepulse amplitude $a_0 = 3.6$). Here, we see that already the prepulse forms its own cavity and the main pulse propagates inside it. As the prepulse has lower amplitude than the main pulse the acceleration is less efficient. Furthermore, what is worse, the prepulse quickly extincts and the cavity starts to be driven by the main pulse, which makes the whole process less stable and hence less efficient. As a result, the attained energies of the electrons are somewhat lower so they emit less photons with lower energies.

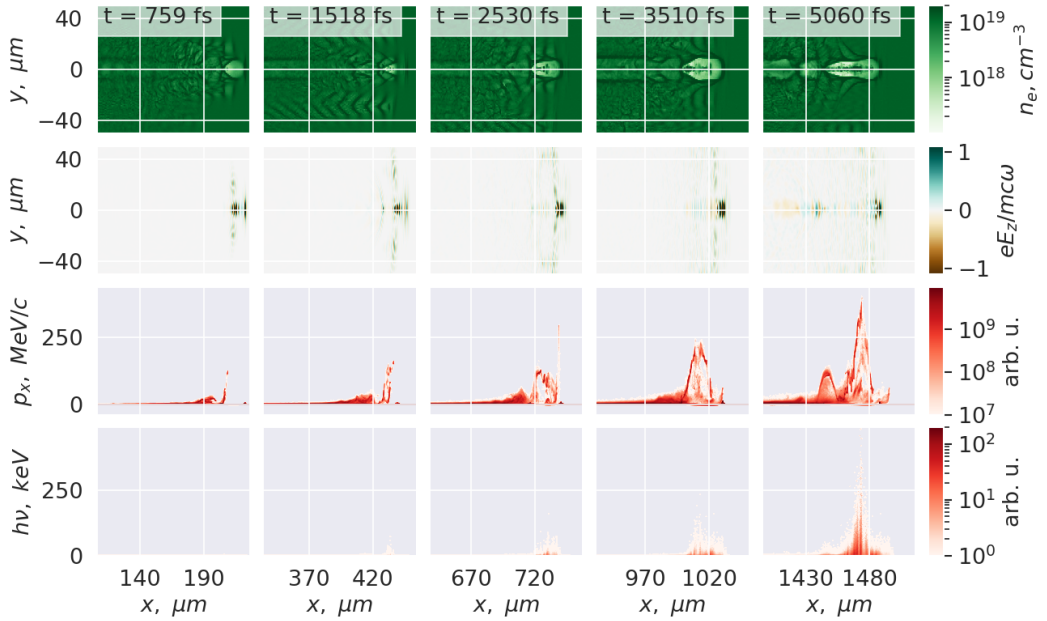

Figure 7. Simulation results for a Gaussian laser pulse with a duration of 11 fs with a 5-fs prepulse. The amplitude of the main pulse is $a_0 = 6.5$ and the amplitude of the prepulse is $a_0 = 3.6$. The data shown is similar to Figure 1.

We would like to underline that even when the prepulse amplitude is as high as $a_0 = 3.6$ its energy is still low compared to the main pulse due to the difference in duration: the prepulse contains only ∼20% of total laser energy in this case. It means that the femtosecond prepulse can significantly affect the acceleration process and betatron radiation even having small energy but concentrated in short pulse.

In the next series of calculations, the effect of a postpulse on the acceleration process was studied. Just as in the case of the prepulse, both the main pulse and the postpulses in these calculations had a Gaussian shape, the main pulse duration was 11 fs, and the postpulse duration was 5 fs. We varied both the postpulse amplitude and the delay between it and the main pulse but did not find any significant influence of the postpulse on the generated photon spectra. Figure 8 shows those spectra for different delays in the case of the postpulse amplitude $a_0 = 3.6$. It somewhat contradicts our expectations as it is known that the pulse overlaping with the accelerated electrons can enhance their transverse oscillations and hence their radiation [28]. We attribute the absence of this effect to the fact that the postpulse in our case has much shorter duration than the electron bunch so it was able to influence insignificantly small fraction of the electrons.

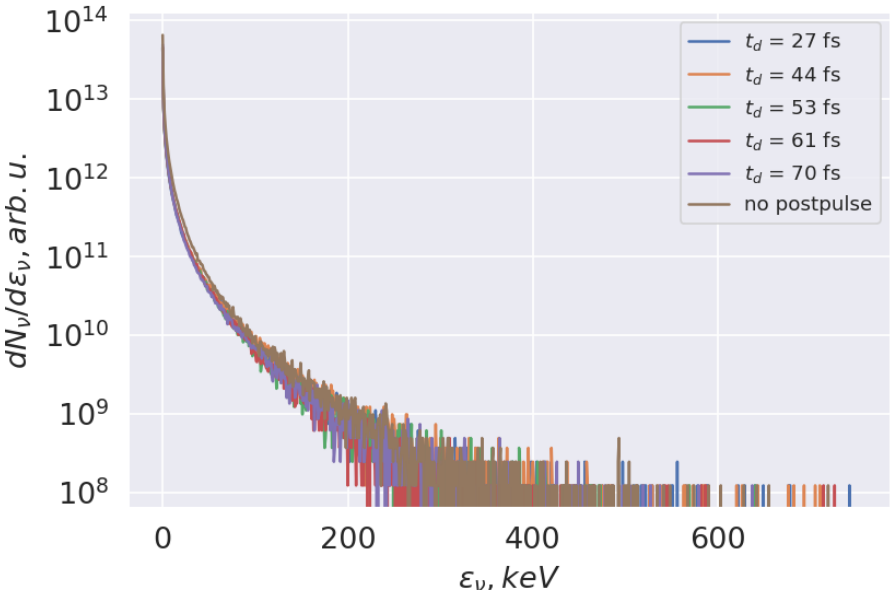

Figure 8. Comparison of photon spectra obtained from the simulations for 11 fs laser pulses with 5 fs postpulses following the main pulse at different delays. In all simulations the main pulse amplitude was $a_0 = 6.5$ and the postpulse amplitude was $a_0 = 3.6$ except the case without postpulse shown for reference in which the main pulse amplitude was $a_0 = 7.5$.

Finally, we studied the influence of a femtosecond pedestal on the interaction process. In this series of calculations, the main pulse had a Gaussian shape and a duration of 11 fs. The pedestal also had a Gaussian shape, and its duration was 50 fs. The centers of the main pulse and the pedestal coincided. We varied the amplitudes of both the main pulse and the pedestal keeping total laser energy constant and equal to 1.73 J. Similarly to the case of prepulse, we found that the pedestal with amplitudes $a_0 < 1$ does not affect the acceleration and radiation process. However, contrary to the prepulse case for higher amplitudes the pedestal never enhance the radiation brightness. The comparison of typical spectra obtained in the case of pedestal with the case of pure pulse is shown in Figure 9. The main reason for the detrimental effect in this case is that the long pedestal contains lot of energy and when its amplitude is $a_0 = 1.1$ the amplitude of the main pulse is as low as $a_0 = 2.5$ whereas the betatron radiation brightness is known to decrease with decreasing pulse intensity.

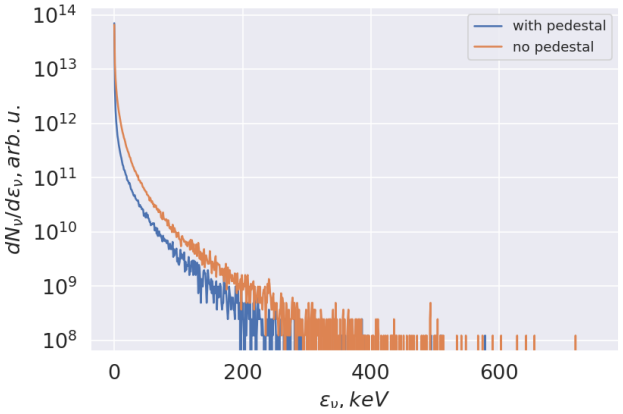

Figure 9. Comparison of photon spectra obtained from the simulations for 11 fs laser pulses with and without 50 fs pedestal. The pedestal amplitude was $a_0 = 1.1$. The main pulse amplitude was $a_0 = 2.5$ in the case with the pedestal and $a_0 = 7.5$ in the case without the pedestal.

4. Discussion

Our study shows that the femtosecond structure of a laser pulse can have a significant effect on its interaction with underdense plasmas. The presence of prepulses can lead to the excitation of plasma wakes that interfere with the wake from the main pulse. In some cases it leads to a more stable interaction dynamics which results in wider emitted photon spectra and its higher brightness. For sufficiently intense prepulses, however, the plasma cavities excited by them and by the main pulse interfere, leading to inhibition of the acceleration process and less efficient betatron radiation. The prepulse containing less than 20% of the energy can either increase maximal energy of generated photons by 50% or at least halve it depending on its amplitude. Simultaneously, the brightness at given photon energy can vary by several times.

Our study did not find any significant effect of the postpulses on the interaction process. The pedestal were shown to inhibit the betatron radiation but only when having amplitudes higher than the relativistic one and the inhibition is due to dramatic decrease in the main pulse amplitude due to presumed constancy of total laser energy.

It should be noted that in experiments the focusing properties of the various components of the pulse also play an important role. Due to the dependence of the nonlinear phase acquiring during the self-phase modulation on the local amplitude of the wave, the structure of the phase front for the main pulse, prepulses, and pedestal can differ significantly, which will lead to an effective decrease in the amplitude of the prepulses and the pedestal at the focus [16,29]. This effect should be taken into account for a more accurate description of the interaction process.

In conclusion, taking into account the femtosecond structure of ultrashort laser pulses obtained by compression after nonlinear self-phase modulation in thin plates can be important in interpreting the results of their interaction with matter, in particular, in the problem of generating betatron radiation by laser wakefield accelerated electrons.

Author Contributions: Conceptualization, A.V.K.; simulations, A.D.S.; writing—original draft preparation, A.V.K.; writing—review and editing, A.D.S.; funding acquisition, A.V.K. All authors have read and agreed to the published version of the manuscript.

Funding: This research was funded by the Ministry of Science and Higher Education of the Russian Federation (Agreement No. 075-15-2021-1361).

Institutional Review Board Statement: Not applicable.

Informed Consent Statement: Not applicable.

Data Availability Statement: The data presented in this study are available on request from the corresponding author.

Acknowledgments: The simulations were performed on resources provided by the Joint Supercomputer Center of the Russian Academy of Sciences.

Conflicts of Interest: The authors declare no conflict of interest. The funders had no role in the design of the study; in the collection, analyses, or interpretation of data; in the writing of the manuscript; or in the decision to publish the results.

Abbreviation

The following abbreviations are used in this manuscript:

FWHM	Full Width at Half Maximum

References

1. Seeck, O.; Murphy, B. *X-ray Diffraction: Modern Experimental Techniques*; Pan Stanford Publishing: Redwood City, CA, USA , 2015.
2. Sanchez-Cano, C.; Alvarez-Puebla, R.A.; Abendroth, J.M.; Beck, T.; Blick, R.; Cao, Y.; Caruso, F.; Chakraborty, I.; Chapman, H.N.; Chen, C.; et al. X-ray-based techniques to study the nano–bio interface. *ACS Nano* **2021**, *15*, 3754–3807. [CrossRef] [PubMed]

3. Banerjee, S.; Chen, S.; Powers, N.; Haden, D.; Liu, C.; Golovin, G.; Zhang, J.; Zhao, B.; Clarke, S.; Pozzi, S.; et al. Compact source of narrowband and tunable X-rays for radiography. *Nucl. Instrum. Methods Phys. Res. Sect. B Beam Interact. Mater. Atoms* **2015**, *350*, 106–111. [CrossRef]
4. Flegentov, V.; Safronov, K.; Gorokhov, S.; Tishchenko, A.; Kovaleva, S.; Potapov, A.; Pavlenko, A. Pulsed laser-plasma gamma radiation source for radiography. *Quantum Electron.* **2021**, *51*, 866–872. [CrossRef]
5. Davis, T.J.; Gao, D.; Gureyev, T.E.; Stevenson, A.W.; Wilkins, S.W. Phase-contrast imaging of weakly absorbing materials using hard X-rays. *Nature* **1995**, *373*, 595–598. [CrossRef]
6. Najmudin, Z.; Kneip, S.; Bloom, M.S.; Mangles, S.P.D.; Chekhlov, O.; Dangor, A.E.; Döpp, A.; Ertel, K.; Hawkes, S.J.; Holloway, J.; et al. Compact laser accelerators for X-ray phase-contrast imaging. *Philos. Trans. R. Soc. A Math. Phys. Eng. Sci.* **2014**, *372*, 20130032. [CrossRef]
7. Corde, S.; Ta Phuoc, K.; Lambert, G.; Fitour, R.; Malka, V.; Rousse, A.; Beck, A.; Lefebvre, E. Femtosecond X rays from laser-plasma accelerators. *Rev. Mod. Phys.* **2013**, *85*, 1. [CrossRef]
8. Albert, F.; Thomas, A.G.R.; Mangles, S.P.D.; Banerjee, S.; Corde, S.; Flacco, A.; Litos, M.; Neely, D.; Vieira, J.; Najmudin, Z.; et al. Laser wakefield accelerator based light sources: Potential applications and requirements. *Plasma Phys. Control. Fusion* **2014**, *56*, 084015. [CrossRef]
9. Umstadter, D.P. All-laser-driven Thomson X-ray sources. *Contemp. Phys.* **2015**, *56*, 417–431. [CrossRef]
10. Esarey, E.; Shadwick, B.A.; Catravas, P.; Leemans, W.P. Synchrotron radiation from electron beams in plasma-focusing channels. *Phys. Rev. E* **2002**, *65*, 056505. [CrossRef]
11. Kostyukov, I.; Kiselev, S.; Pukhov, A. X-ray generation in an ion channel. *Phys. Plasmas* **2003**, *10*, 4818–4828. [CrossRef]
12. Kiselev, S.; Pukhov, A.; Kostyukov, I. X-ray generation in strongly nonlinear plasma waves. *Phys. Rev. Lett.* **2004**, *93*, 135004. [CrossRef] [PubMed]
13. Albert, F.; Thomas, A.G.R. Applications of laser wakefield accelerator-based light sources. *Plasma Phys. Control. Fusion* **2016**, *58*, 103001. [CrossRef]
14. Lu, W.; Tzoufras, M.; Joshi, C.; Tsung, F.; Mori, W.; Vieira, J.; Fonseca, R.; Silva, L. Generating multi-GeV electron bunches using single stage laser wakefield acceleration in a 3D nonlinear regime. *Phys. Rev. Spec. Top.-Accel. Beams* **2007**, *10*, 061301. [CrossRef]
15. Gordienko, S.; Pukhov, A. Scalings for ultrarelativistic laser plasmas and quasimonoenergetic electrons. *Phys. Plasmas* **2005**, *12*, 043109. [CrossRef]
16. Khazanov, E.A.; Mironov, S.Y.; Mourou, G. Nonlinear compression of high-power laser pulses: Compression after compressor approach. *Phys.-Uspekhi* **2019**, *62*, 1096. [CrossRef]
17. Ginzburg, V.N.; Yakovlev, I.V.; Zuev, A.S.; Korobeynikova, A.P.; Kochetkov, A.A.; Kuz'min, A.A.; Mironov, S.Y.; Shaykin, A.A.; Shaykin, I.A.; Khazanov, E.A. Compression after compressor: Threefold shortening of 200-TW laser pulses. *Quantum Electron.* **2019**, *49*, 299–301. [CrossRef]
18. Ginzburg, V.N.; Yakovlev, I.V.; Zuev, A.S.; Korobeynikova, A.P.; Kochetkov, A.A.; Kuzmin, A.A.; Mironov, S.Y.; Shaykin, A.A.; Shaikin, I.A.; Khazanov, E.A. Two-stage nonlinear compression of high-power femtosecond laser pulses. *Quantum Electron.* **2020**, *50*, 331–334. [CrossRef]
19. Ginzburg, V.; Yakovlev, I.; Zuev, A.; Korobeynikova, A.; Kochetkov, A.; Kuzmin, A.; Mironov, S.; Shaykin, A.; Shaikin, I.; Khazanov, E.; et al. Fivefold compression of 250-TW laser pulses. *Phys. Rev. A* **2020**, *101*, 013829. [CrossRef]
20. Mironov, S.Y.; Fourmaux, S.; Lassonde, P.; Ginzburg, V.N.; Payeur, S.; Kieffer, J.C.; Khazanov, E.A.; Mourou, G. Thin plate compression of a sub-petawatt Ti:Sa laser pulses. *Appl. Phys. Lett.* **2020**, *116*, 241101. [CrossRef]
21. Shaykin, A.; Ginzburg, V.; Yakovlev, I.; Kochetkov, A.; Kuzmin, A.; Mironov, S.; Shaikin, I.; Stukachev, S.; Lozhkarev, V.; Prokhorov, A.; et al. Use of KDP crystal as a Kerr nonlinear medium for compressing PW laser pulses down to 10 fs. *High Power Laser Sci. Eng.* **2021**, *9*, e54. [CrossRef]
22. Kim, J.I.; Kim, Y.G.; Yang, J.M.; Yoon, J.W.; Sung, J.H.; Lee, S.K.; Nam, C.H. Sub-10 fs pulse generation by post-compression for peak-power enhancement of a 100-TW Ti:Sapphire laser. *Opt. Express* **2022**, *30*, 8734–8741. [CrossRef] [PubMed]
23. Ginzburg, V.; Yakovlev, I.; Kochetkov, A.; Kuzmin, A.; Mironov, S.; Shaikin, I.; Shaykin, A.; Khazanov, E. 11 fs, 1.5 PW laser with nonlinear pulse compression. *Opt. Express* **2021**, *29*, 28297. [CrossRef]
24. Fourmaux, S.; Lassonde, P.; Mironov, S.Y.; Hallin, E.; Légaré, F.; Maclean, S.; Khazanov, E.A.; Mourou, G.; Kieffer, J.C. Laser wakefield acceleration based x ray source using 225-TW and 13-fs laser pulses produced by thin film compression. *Opt. Lett.* **2022**, *47*, 3163. [CrossRef] [PubMed]
25. Maslov, V.; Bondar, D.; Grigorencko, V.; Levchuk, I.; Onishchenko, I. Control of Characteristics of Self-Injected and Accelerated Electron Bunch in Plasma by Laser Pulse Shaping on Radius, Intensity and Shape. *Probl. At. Sci. Technol.* **2019**, *124*, 39–42. [CrossRef]
26. Surmin, I.A.; Bastrakov, S.I.; Efimenko, E.S.; Gonoskov, A.A.; Korzhimanov, A.V.; Meyerov, I.B. Particle-in-Cell laser-plasma simulation on Xeon Phi coprocessors. *Comput. Phys. Commun.* **2016**, *202*, 204–210. [CrossRef]
27. Gonoskov, A.; Bastrakov, S.; Efimenko, E.; Ilderton, A.; Marklund, M.; Meyerov, I.; Muraviev, A.; Sergeev, A.; Surmin, I.; Wallin, E. Extended particle-in-cell schemes for physics in ultrastrong laser fields: Review and developments. *Phys. Rev. E* **2015**, *92*, 023305. [CrossRef]

28. Zhang, X.; Khudik, V.N.; Shvets, G. Synergistic Laser Wakefield/Direct Laser Acceleration in the Plasma Bubble Regime. *Phys. Rev. Lett.* **2015**, *114*, 184801. [CrossRef]
29. Martyanov, M.; Mironov, S.; Starodubtsev, M.; Soloviev, A.; Kochetkov, A.; Ginzburg, V.; Shaikin, A.; Khazanov, E. Improvement of the focusability of petawatt laser pulses after nonlinear post-compression. *J. Opt. Soc. Am. B* **2022**, *39*, 1936. [CrossRef]